Enhanced Modulation Technique for Power Quality Improvement of LED Drivers

Huan Li
School of Electrical and Information Engineering
The University of Sydney
Sydney, Australia
huan.li@sydney.edu.au

Weidong Xiao
School of Electrical and Information Engineering
The University of Sydney
Sydney, Australia
weidong.xiao@sydney.edu.au

Sinan Li
School of Electrical and Information Engineering
The University of Sydney
Sydney, Australia
sinan.li@sydney.edu.au

Jimmy Chih-Hsien Peng
Department of Electrical and Computer Engineering
National University of Singapore
Singapore, Singapore
jpeng@nus.edu.sg

2021 IEEE Energy Conversion Congress and Exposition (ECCE) | 978-1-7281-5135-9/21/$31.00 ©2021 IEEE | DOI: 10.1109/ECCE47101.2021.9594938

***Abstract*—Light-emitting diode (LED) tends to be the lighting source in the future. With the increasing utilization, the accumulating power capacity brings the grid impact into attention. A LED driver is required to maintain good input power quality to minimize any negative impact on grid. In this paper, a novel modulation technique is proposed to enhance power quality. First, a current reference for hysteresis control is optimally derived for AC current to follow the ideal sinusoidal waveform and maintain power factor. Furthermore, the proposed adaptive band-gap control method maintains steady switching frequency, which eases the filter design and component selection. Simulation and experiment verified the advantages that the proposed methodology maintain good power quality, maintains steady switching operation, and achieves high efficiency.**

***Index Terms*—LED drivers, hysteresis control, power factor correction, total harmonic distortion, adaptive band-gap.**

I. Introduction

Light-emitting diodes (LEDs) show advantages of mercury free, high efficacy, long lifespan and fast response in comparison with other existing lighting technologies, [1]. Drivers are essential to provide regulated power to LEDs for long lifespan [2]. LEDs are widely supplied by single-phase AC in home and office. When the power capacity reaches a certain level, the power factor correction (PFC) enforced by electric codes or standards, such as IEC61000-3-2 to minimize low harmonic distortion, [3], [4].

LED driver topologies are typically classified as the two-stage and single-stage, as shown in Fig. 1. The two-stage shows the cascaded two DC/DC converters. One performs the PFC, and another regulate the current to drive LEDs. One DC link is required for power flow. The single-stage LED driver uses only one converter to perform both PFC and output current regulation and shows the advantage of simplicity. Traditionally, significant capacitance is required for the output filter to reduce both double-line frequency ripple to maintain DC power quality to drive LEDs. One study shows that the 100 Hz or 120 Hz flicker is invisible to human eyes if low capacitance is only applied to filter the switching frequency instead of double-line frequency, [5]. Furthermore, there is no evidence that the pulsating output current will accelerate degradation of LEDs as long as the peak-to-average ratio is not too high, as claimed in [6], [7].

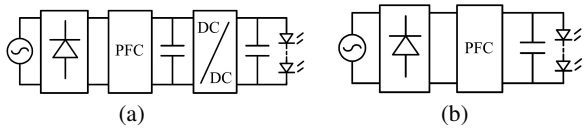

Fig. 1. LED driver configurations: (a) cascaded two-stage; (b) single-stage.

For single-stage LED drivers, the buck topology is widely utilized because of its simplicity, high efficiency and step-down feature [8], [9]. To achieve the PFC and current regulation, the average-current-mode (ACM) control is widely adopted, where the current is sensed and regulated to follow a reference signal by either hysteresis control or peak-current control. The hysteresis control technique shows higher control accuracy than the peak-current control [10], but the switching frequency of AC/DC converter under the traditional hysteresis control may grows rapidly during the peak period of input voltage, which makes switch selection and filter design difficult. Besides, the control performance of hysteresis control is very sensitive to delay caused by sensing, controller and gate driver.

Two important factors, reference signal and control technique, determine the performance of ACM control. One study recommends the reference signal is formed by the SIN waveform to achieve the desired PFC, [11]. It is also suggested to utilize the SIN^2 reference because the LED behaves more like a constant voltage load, [12]. The total harmonic distortion (THD) can be reduced accordingly. However, modeling LED as a constant voltage load is not precise, [13]. The model of LEDs is different from conventional loads. When the

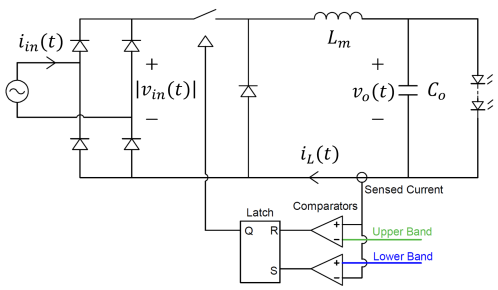

Fig. 2. Typical hysteresis controller design of single-stage LED driver.

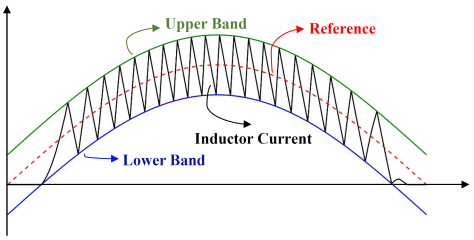

Fig. 3. Typical corresponding waveform of inductor current waveform.

LED model is accurately derived, an improved modulation technique can be developed for the optimal reference and control, which eventually reduce the total harmonic distortion and improve power quality, [14].

In this paper, we further improve the method in [14] and provide more experimental results for performance evaluation and comparison. A modified hysteresis control based on adaptive band-gap is proposed to track the reference, which improves power factor, enables a constant switching frequency, and simplifies the design of low-pass filter. Although the output current contains significant double-line frequency ripple, a small film capacitor can be used as the output filter to improve the reliability of the proposed LED driver and the proposed technique can be used in the applications where flicker is not of primary concern such as parking lots and signal lights.

II. Driver Circuit and Proposed Modulation

Fig. 2 provides a typical design of buck converter with the hysteresis controller and the inductor current regulation. The inductor current waveform shall be regulated into sinusoidal form, as illustrated in Fig. 3. The upper bound and lower bound is usually pre-defined in a look-up table of control integrated circuit or generated at real time by micro-controllers. In this section, the relationship between the current reference,$i_{ref}(t)$, the band-gap, $\Delta i(t)$, and the input power, $p_{in}(t)$, is analyzed. The analysis leads to the optimization for high power quality.

A. Varying Switching Period

This section focuses on the mathematic model between switching period and other design parameters to study how the variation of switching frequency comes from and how to eliminate the variation. The switching frequency in the

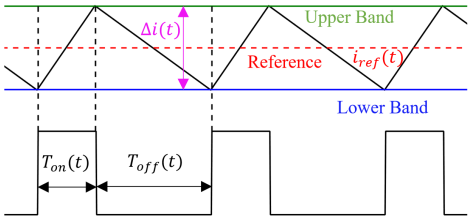

Fig. 4. Inductor current waveform of hysteresis control with high switching frequency.

hysteresis control scheme is inconstant because the input voltage is shaped from the sine wave with the double-line frequency. Since the reference signal, $i_{ref}(t)$, the input voltage, $V_{in}sin\omega t$, and the adaptive bandgap, $\Delta i(t)$, are varying at the frequency that is much lower than the switching frequency, they can be assumed as a constant value within each switching cycle, as demonstrated in Fig. 4.

When the switch is turned on for conduction, the rising slope of the inductor current becomes

$$k_{on}(t) = \frac{V_{in}|sin\omega t| - v_o(t)}{L_m} \tag{1}$$

where $v_o(t)$ is the output voltage. Thus, the on-time $T_{on}(t)$, can be calculated as

$$T_{on}(t) = \frac{\Delta i(t)}{k_{on}(t)} = \frac{L_m \Delta i(t)}{V_{in}|sin\omega t| - v_o(t)}. \tag{2}$$

When the switch is turned off, the current slope becomes

$$k_{off}(t) = -\frac{v_o(t)}{L_m}. \tag{3}$$

Then, the off-time, $T_{off}(t)$, is calculated as

$$T_{off}(t) = -\frac{\Delta i(t)}{k_{off}(t)} = \frac{L_m \Delta i(t)}{v_o(t)}. \tag{4}$$

So the switching period , $T_s(t)$, is derived as

$$T_s(t) = T_{on}(t) + T_{off}(t) = \frac{L_m V_{in} \Delta i(t)}{V_{in} v_o(t) - \frac{v_o(t)^2}{|sin\omega t|}}. \tag{5}$$

Therefore, $T_s(t)$ varies with $|sin\omega t|$ when the traditional hysteresis control with fixed band-gap is applied. The adaptive adjustment of $\Delta i(t)$ can compensate the variation of the switching frequency brought by $v_o(t)$ and $|sin\omega t|$.

B. Average Input Power Within Each Switching Period

The reference signal for the inductor current can be optimized in the hysteresis control to perform PFC. The cycle to cycle analysis is performed to analyze the relationship between inductor current, $i_L(t)$, and input power, $p_{in}(t)$, such that the current reference could be designed to achieve superior input power quality. When the switch is turned on, the input current is exactly the inductor current which is

$$i_{in}(t) = i_L(t) = i_{ref}(t) - \frac{1}{2}\Delta i(t) + k_{on}(t)t. \tag{6}$$

Therefore, the input power is determined as (7) when the switch turns on.

$$p_{in}(t) = i_{in}(t)V_{in}sin\omega t \tag{7}$$

$$p_{in}(t) = (i_{ref}(t) - \frac{1}{2}\Delta i(t) + k_{on}(t)t)V_{in}sin\omega t. \tag{8}$$

The $p_{in}(t)$ remains zero when the switch turns off. Thus, the average input power within a switching period, $p_{av}(t)$, is derived as

$$p_{av}(t) = \frac{T_{on}(t)(i_{ref}(t) - \frac{1}{2}\Delta i(t) + k_{on}(t)t)V_{in}|sin\omega t|}{T_s(t)} \tag{9}$$

Substituting (1), (2), and (5) into (8), the $p_{av}(t)$ is further derived to be

$$p_{av}(t) = i_{ref}(t)v_o(t) \tag{10}$$

According to (9), the input power is not only dependent on the current reference but also the V-I characteristics of the load.

III. Current Reference And Adaptive Band-gap

This section describes the proposed modulation method to enhance power quality for LED drivers.

A. Proposed Current Reference

The PFC regulates the input current to be shaped and proportional to the AC voltage, which is expressed by $I_{in}sin\omega t$. Thus, the $p_{av}(t)$ should be regulated as

$$p_{av}(t) = 2P_o sin^2\omega t \tag{11}$$

where P_o is the DC component of the output power. Thus, according to (9), the reference signal should be set as

$$i_{ref}(t) = \frac{2P_o sin^2\omega t}{v_o(t)}. \tag{12}$$

With the output capacitor for filtering, the output load current can be approximated as the reference inductor current $i_{ref}(t)$. For pure resistive load, the output voltage is

$$v_o(t) = Ri_{ref}(t) \tag{13}$$

where R is the load resistance. Substituting (12) into (11), the current reference for a pure resistive load is derived to be (13), which is called as SIN modulation.

$$i_{ref}(t) = \sqrt{\frac{2P_o}{R}}sin\omega t. \tag{14}$$

For constant voltage load, the output voltage is constant at V_o. The current reference is calculated as (14), which is referred to SIN^2 modulation.

$$i_{ref}(t) = \frac{2P_o}{V_o}sin^2\omega t. \tag{15}$$

The I-V characteristics of LEDs can be modelled as the equivalent circuit of a diode with threshold voltage V_F in series connection with a resistor, r_{LED}, as shown in Fig. 5. Therefore, the voltage across a LED can be calculate as

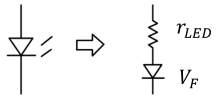

Fig. 5. Linearized electric model of LED.

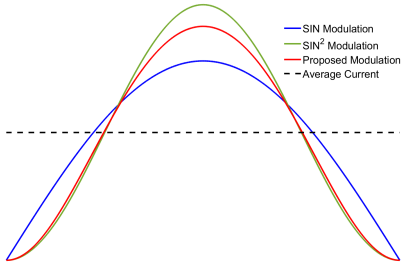

Fig. 6. Current references of SIN modulation, SIN^2 modulation and the proposed modulation (V_F=2.5V and r_{LED}=2.5 Ω.

$$v_o(t) = r_{LED}i_{ref}(t) + V_F. \tag{16}$$

Thus, $i_{ref}(t)$ should be assigned as (16) for the best match of sinusoidal AC and ideal power quality.

$$i_{ref}(t) = \frac{2P_o sin^2\omega t}{r_{LED}i_{ref}(t) + V_F}. \tag{17}$$

Solving (16) leads to the proposed reference for LED driver, expressed by

$$i_{ref}(t) = \sqrt{\frac{2P_o}{r_{LED}}sin^2\omega t + \frac{V_F^2}{4r_{LED}^2}} - \frac{V_F}{2r_{LED}}. \tag{18}$$

Fig. III-A compares the amplitude of the proposed modulation with SIN modulation and SIN^2 modulation with consideration of V_F = 2.5V and r_{LED} = 2.5 Ω for a typical LED cell. The proposed modulation shows lower peak-to-average than SIN^2 modulation and reduces the current stress of the whole circuit.

B. Adaptive Band-gap for Constant Switching Frequency

The early analysis shows that the switching period is varying under traditional fixed band-gap hysteresis control. To fix this problem, the main idea is to vary the band-gap to compensate the variation. Reorganizing (5) and the band-gap is

$$\Delta i(t) = \frac{v_o(t)(V_{in}|sin\omega t| - v_o(t))}{f_{sw}(t)L_m V_{in}|sin\omega t|} \tag{19}$$

where $f_{sw}(t)$is the varying switching frequency. Substituting (15) into (18) and assuming the switching frequency to be constant, the adaptive band-gap can be derived as

$$\Delta i(t) = \frac{v_o(t)(V_{in}|sin\omega t| - r_{LED}i_{ref}(t) - V_F)}{f_{sw}L_m V_{in}|sin\omega t|}. \tag{20}$$

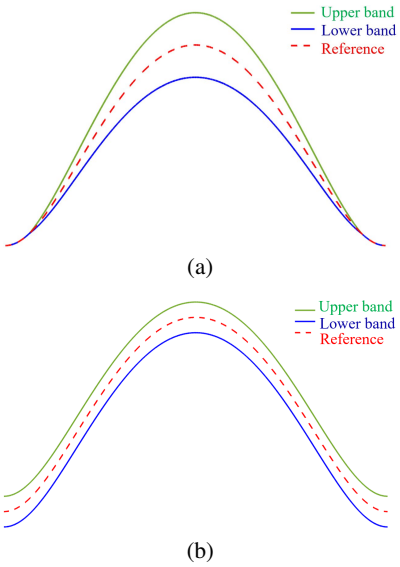

Fig. 7. Comparison between: (a) proposed modulation with adaptive band-gap; (b) traditional modulation based on fixed band-gap.

To track the reference and maintain steady switching, the mathematic expression of upper band and lower band are therefore set as

$$i_{upper}(t) = i_{ref}(t) + \frac{1}{2}\Delta i(t). \tag{21}$$

$$i_{lower}(t) = i_{ref}(t) - \frac{1}{2}\Delta i(t). \tag{22}$$

The difference between the conventional fixed-band hysteresis control and the proposed adaptive-band hysteresis control is illustrated in Fig. 7. It can be seen that the proposed modulation shows narrower band-gap when the input voltage is low to maintain switching frequency. When the input voltage is high, the proposed modulation increases the band-gap to prevent the switching frequency from exceeding the design value. Thus, the switching capability of switch is fully utilized, meanwhile the power quality at the zero crossing is improved.

IV. Verification

The concept proof is conducted through both simulation and experimental evaluation.

A. Simulation

The simulation waveforms of the input current under SIN, SIN^2, and proposed modulation schemes are shown in Fig.8. According to the waveforms of simulation, the input current matches better with the sine wave when the proposed method is applied. The THD values of different modulation methods are summarized in Table II showing the simulation results.

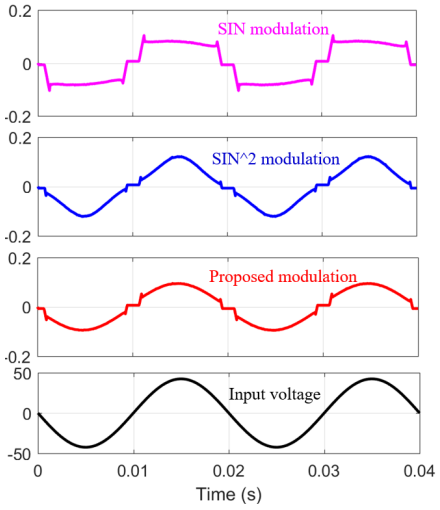

Fig. 8. Simulation results of input current under SIN, SIN^2 and proposed modulation, respectively.

B. Experiment

Table I summarizes the design parameters of the prototype. The measured waveforms are shown in Fig. 9, which are used to compare different modulation methods regarding SIN, SIN^2, and the proposed solutions. It shows that the proposed reference significantly reduces the third order harmonic. The THD values of different modulation methods are summarized in Table II showing the experimental results. The proposed modulation delivered the lowest THD level as expected.

TABLE I
Design Parameters

Symbol	Parameter	Value
$V_{in\cdot RMS}$	RMS value of input voltage	220V
I_o	Average output current	350mA
f_{sw}	switching frequency	100kHz
$\Delta i(t)$	Fixed band-gap	80mA
L_m	Output inductor	4mH
C_o	Output capacitor	3.3 μF
V_F	Forward voltage	60V
r_{LED}	Load resistance	40 Ω

The dimming waveform is shown in Fig. 10. Traditionally, the timing for dimming should happen at the zero-crossing period of the input voltage to achieve soft transition and higher input quality. However, the timing for dimming is intentionally selected during the peak period of input voltage to demonstrate the superior dynamics performance and inherent current limitation of hysteresis control as illustrated in Fig. 10.

The comparison was also made between the traditional hysteresis control based on fixed band-gap and the proposed with adaptive band-gap. The fixed band-gap was set at 80mA such that the switching frequency was fluctuating around 100kHz. The adaptive band-gap was set to maintain the switching at 100kHz. Fig. 11 shows the inductor current under the proposed modulation and the traditional hysteresis control. During the peak period of input voltage, the switching frequency under

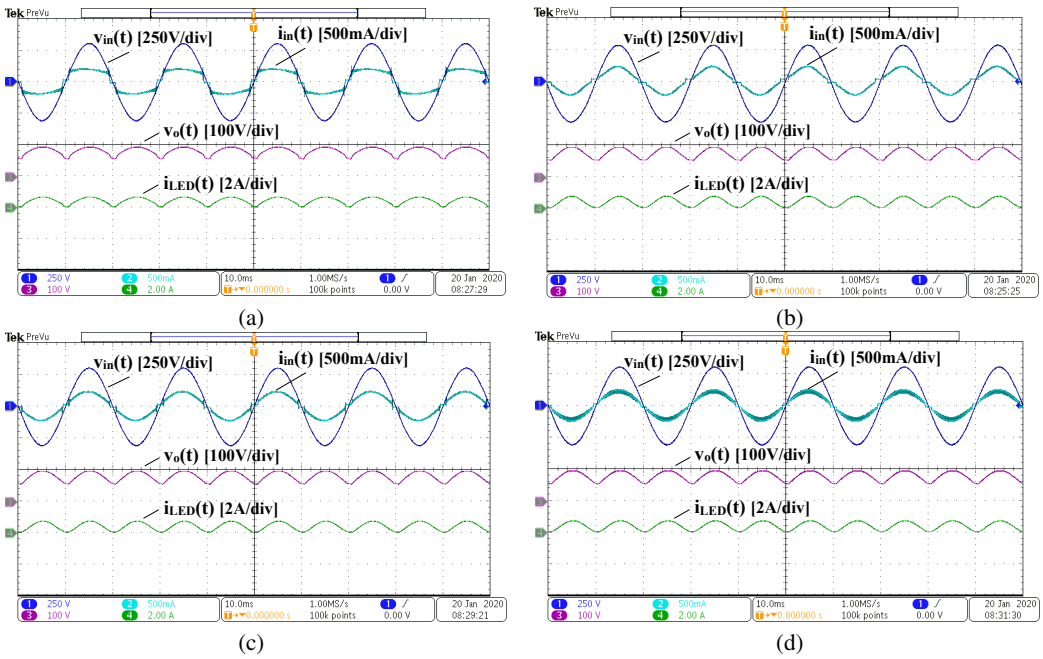

Fig. 9. Key experimental waveforms of the prototype design: (a) SIN reference (fixed band-gap); (b) SIN^2 reference (fixed band-gap); (c)Proposed reference (fixed band-gap); (d) Proposed reference (adaptive band-gap).

TABLE II
THD VALUES OF DIFFERENT MODULATION METHODS

Modulation	THD value
SIN (simulation)	26%
SIN^2 (simulation)	15%
Proposed method (simulation)	7%
SIN (Experimental test)	25%
SIN^2 (Experimental test)	15%
Proposed modulation (Experimental test)	8%

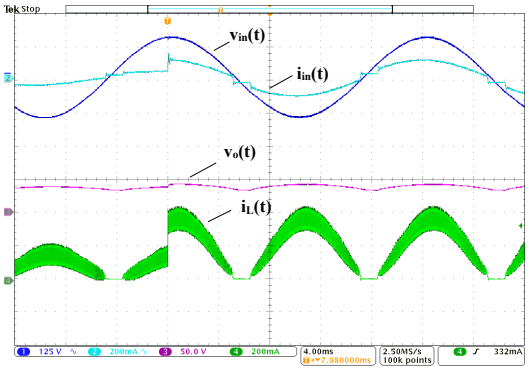

Fig. 10. Sudden reference variation to evaluate dimming performance.

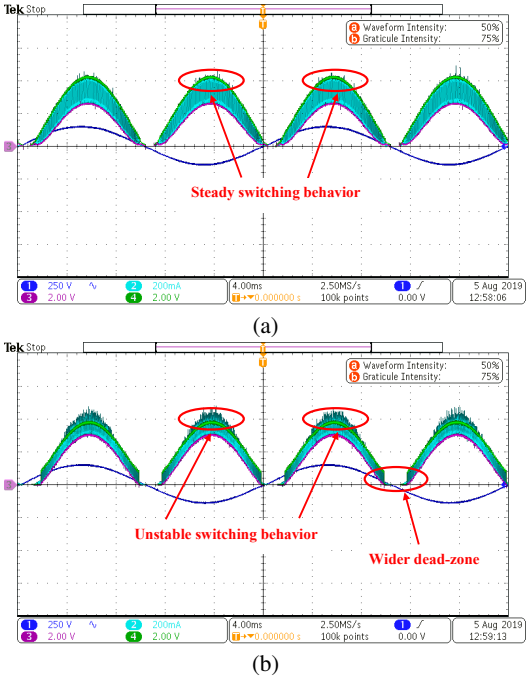

Fig. 11. Inductor current, upper band and lower band of: (a) proposed adaptive band-gap. (b) traditional hysteresis control.

traditional hysteresis control grows rapidly and the inductor current cannot be well maintained between the upper band and lower band as shown in Fig. 11 (b). Comparing with the traditional hysteresis control, the proposed hysteresis control can well stabilize the switching behavior and is less sensitive to propagation delay, which results in better control performance as shown in Fig. 11 (a). The Fig. 12 shows the harmonics spectrum of gate signal under conventional hysteresis control and proposed adaptive band-gap modulation. It verified that the

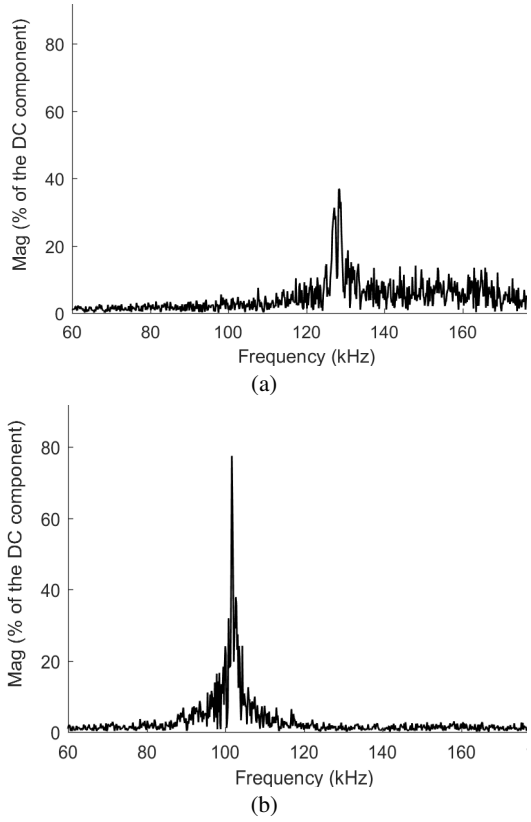

Fig. 12. Harmonic spectrum of gate signal: (a) under the traditional hysteresis control; (b) Under the proposed adaptive band-gap modulation.

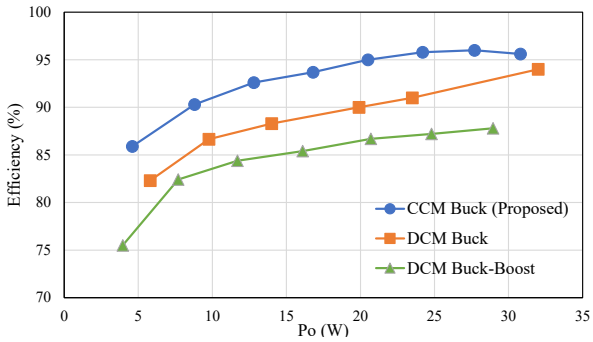

Fig. 13. Efficiency of the prototypes with respect to different power level.

proposed method can maintain the switching frequency at a constant level and thus prevents the switching frequency from exceeding its maximum value. The efficiency curve is shown in Fig. 13. The proposed driver shows the highest efficiency when it is operated at CCM. For comparison, the efficiency curve is added when the prototype operate at DCM. Based on the same power rating, a buck-boost converter is included for the comparison when it is modulated for DCM.

V. Conclusion

This paper presented a novel modulation technique based on hysteresis control for single-stage buck-based LED driver. The enhancement of input power quality results from a new derivation of the current reference and accurate regulation of the output current. An adaptive band-gap modulation is also proposed in maintaining constant switching. Both simulation and experiment are used to prove the theoretical analysis and practical effectiveness. The experimental results show that the proposed method significantly reduces the distortion of input current especially the third order harmonic. The frequency spectrum of the gate signal verifies that the switching frequency is well controlled at the steady level always under the upper limit. Thus, the switching capability can be fully utilized. The proposed modulation is practical for implementation since it can be easily implemented on existing hysteresis control integrated circuits by updating the look-up table of current reference and does not require any extra logic components.

References

[1] H. Li, S. Li, and W. Xiao, "Single-Phase LED driver with reduced power processing and power decoupling," IEEE Transactions on Power Electronics, vol. 36, pp. 4540-4548, Apr. 2021

[2] Y. Wang, J. M. Alonso, and X. Ruan, "A review of led drivers and related technologies," IEEE Transactions on Industrial Electronics, vol. 64, no. 7, pp. 5754–5765, Jul. 2017.

[3] H. Li and W. Xiao, "LED driver based on novel ripple cancellation technique for flicker-free operation and reduced power processing," IET Power Electronics, vol. 13, pp. 3026-3031, Nov. 2020.

[4] S. Li, S. Tan, C. K. Lee, E. Waffenschmidt, S. Y. Hui, and C. K. Tse, "A survey, classification, and critical review of light-emitting diode drivers," IEEE Transactions on Power Electronics, vol. 31, no. 2, pp. 1503–1516, Feb. 2016

[5] A. Wilkins, J. Veitch, and B. Lehman, "Led lighting flicker and potential health concerns: Ieee standard par1789 update," in 2010 IEEE Energy Conversion Congress and Exposition, pp. 171–178, Sep. 2010.

[6] S. Buso, G. Spiazzi, M. Meneghini, and G. Meneghesso, "Performance degradation of high-brightness light emitting diodes under dc and pulsed bias," IEEE Transactions on Device and Materials Reliability, vol. 8, no. 2, pp. 312–322, Jun. 2008

[7] C. Liu, X. Lai, H. He, and H. Du, "Sectional linear led driver for optimised efficiency in lighting applications," IET Power Electronics, vol. 9, no. 4, pp. 825–834, 2016.

[8] X. Qu, S. Wong, and C. K. Tse, "Resonance-assisted buck converter for offline driving of power led replacement lamps," IEEE Transactions on Power Electronics, vol. 2, no. 2, pp. 532–540, Feb. 2011.

[9] W. Xiao. Power Electronics Step-by-Step: Design, Modeling, Simulation, and Control, 1st ed, McGraw-Hill Education, 2021

[10] B. Lim, Y. Ko, Y. Jang, O. Kwon, S. Han, and S. Lee, "A 200-v 98.16improve current accuracy for large-scale single-string led backlighting applications," IEEE Transactions on Power Electronics, vol. 31, no. 9, pp. 6416–6427, Sep. 2016.

[11] C. Shin, W. Lee, S. Lee, S. Lee, J. Bang, S. Hong, and G. Cho, "Sine-reference band (srb)-controlled average current technique for phase-cut dimmable ac-dc buck led lighting driver without electrolytic capacitor," IEEE Transactions on Power Electronics, vol. 33, no. 8, pp. 6994–7009, Aug. 2018.

[12] K. Cho and R. Gharpurey, "An efficient buck/buck-boost reconfigurable led driver employing sin2 reference," IEEE Journal of Solid-State Circuits, vol. 52, no. 10, pp. 2758–2768, Oct. 2017.

[13] Z. Dong, C. K. Tse, and S. Y. R. Hui, "Circuit theoretic considerations of led driving: Voltage-source versus current-source driving," IEEE Transactions on Power Electronics, vol. 34, no. 5, pp. 4689–4702, May. 2019

[14] H. Li, W. Hassan and W. Xiao, "A Novel Current Reference to Enhance Input Power Quality of Single-stage LED Driver," IEEE 4th International Future Energy Electronics Conference (IFEEC), 2019